Journal of Alloys and Compounds 509 (2011) 8013–8017

Contents lists available at ScienceDirect

Journal of Alloys and Compounds

journal homepage: www.elsevier.com/locate/jallcom

Influence of Si and Ti contents on the microstructure, microhardness and performance of TiAlSi intermetallics in Al–Si–Ti alloys

Tong Gao, Pengting Li, Yunguo Li, Xiangfa Liu*

Key Laboratory for Liquid-Solid Structural Evolution and Processing of Materials, Ministry of Education, Shandong University, 17923 Jingshi Road, Jinan 250061, PR China

ARTICLE INFO

Article history:
Received 18 March 2011
Received in revised form 7 May 2011
Accepted 9 May 2011
Available online 26 May 2011

Keywords:
TiAlSi intermetallics
Si content
Microhardness
Morphology
Mechanical properties

ABSTRACT

In this study, the influence of Si and Ti contents on the microstructure, microhardness and morphology of TiAlSi intermetallics in ternary Al–Si–Ti alloys was investigated. The increase of Si addition in Al–*x*Si–2Ti alloys leads to an increase of Si content in TiAlSi phase as well as an increase of microhardness. A phase evolution from $Ti(Al_{1-x}Si_x)_3$ to $Ti_7Al_5Si_{12}$ at about 14 wt.% Si was detected, while all the TiAlSi intermetallics exhibit flake-like. The increase of Ti content promotes the morphological transformation of TiAlSi from flake-like to block-like and primary Si particles are replaced by blocky TiAlSi particles in hypereutectic Al–Si alloy. The high-temperature strengthening effect of TiAlSi particles in a piston alloy was investigated and the strength is increased by 11.9% in this article, while the elongation and yield strength are increased by 17.6% and 10.1%, respectively.

1. Introduction

Al–Si alloys are well-known casting alloys and widely used in many fields, especially for cylinder blocks, cylinder heads, pistons and valve lifters, due to low thermal-expansion coefficient, high wear resistance, good corrosion resistance, and improved mechanical properties [1–3].

Ti is an important element in Al–Si alloy, due to its grain refining role and solution strengthening effect [4–7]. The solubility limit of Ti in α-Al is between 0.12% and 0.15% (all compositions quoted in this work are in wt.% unless otherwise stated), which is the typical level used in grain refined Al–Si alloys [8–10]. However, an excess of Ti may cause problems in the liquid metal process and defects in casting, such as feeding blockage, wormhole defect [9], due to precipitation of primary TiAlSi intermetallics [11].

So far, there are various ternary Al–Si–Ti phase diagrams calculated and updated by lots of researchers [12,13] and the titanium aluminides are commonly studied through thermodynamic calculation. However, the comprehensive investigation of the composition, structure and morphology of TiAlSi intermetallics in Al–Si–Ti alloy through experimental method has been seldom reported. What's more, no agreement has been reached on Ti-containing phase in Al–Si–Ti alloy according to various references. Saheb et al. [11] identified a binary $TiAl_3$ phase, while Chen et al. [9] and Zeren et al. [10,14] found a ternary TiAlSi phase in Al–Si–Ti alloys.

The purpose of the present work is to investigate the composition, phase evolution and microhardness of TiAlSi intermetallics with Si content in Al–*x*Si–2Ti ($3 \le x \le 60$) alloys. The effect of Ti content on the morphology of TiAlSi has been explored, and the effect of blocky TiAlSi particles on high-temperature strength in an Al–Si piston alloy has also been investigated.

2. Experimental

Eight Al–*x*Si–2Ti alloys ($x = 3$, 6, 10, 12, 14, 18, 30 and 60) were prepared using commercial pure Al (99.7%), commercial pure crystalline Si (99.9%) and Ti sponge (99.9%). The alloys were melting in a clean graphite crucible by high frequency induction furnace up to 1200 °C, and were poured into a cast iron chill.

Three Al–18Si–Ti alloys with 2, 4 and 5% Ti were prepared in a clay-bonded graphite crucible heated by 25 kW medium frequency induction furnace to 900 ± 50 °C and were poured into the same cast iron chill mentioned above. Metallographic specimens were all cut from the same position of the casting samples, then mechanically ground and polished in standard routines.

A piston alloy (the compositions are listed in Table 1) was prepared in a clay-bonded graphite crucible heated by 25 kW medium frequency induction furnace at 800 °C. Then 0.5 wt.% of Al–3.5P master alloy was added. After that the melt was carried out using 0.5 wt.% C_2Cl_6 at 800 °C for slag-removing and degassing. Then melt was poured into a pre-heated (200 °C) mold at 780 °C to gain tensile test bars. Another group with extra 3% Ti addition by Al–6Ti master alloy was prepared the same method as above. The two groups are defined as group 1 and 2, respectively.

Test bars were then heat-treated in the process: solution treated at 505 °C for 4 h; water quenched; aging treated at 200 °C for 8 h and cooled in air. The test bars were machined to 'dog-bone' type specimens (Fig. 1), and then

* Corresponding author. Tel.: +86 531 88392006; fax: +86 531 88395414.
E-mail address: xfliu@sdu.edu.cn (X. Liu).

0925-8388/$ – see front matter © 2011 Elsevier B.V. All rights reserved.
doi:10.1016/j.jallcom.2011.05.032

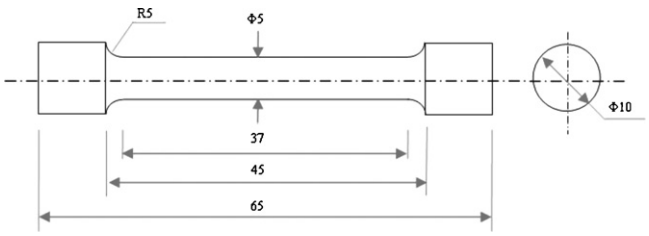

Fig. 1. Pattern dimensions for 'dog-bone' type specimen.

test by electronic all-purpose test machine at 350 °C. The elongation (δ) and yield strength ($\sigma_{p0.05}$) at 350 °C were also tested and shown in Table 1. Each data reported is an average of four tensile specimens. Specimens for metallographic microstructure observation were cut from tensile bars after heat-treatment.

The microstructure analysis was carried out by field emission scanning electron microscopy (FESEM), energy dispersive X-ray spectroscopy (EDS) and X-ray diffraction (XRD). The microhardness of as-cast specimens was measured using a microhardness tester (DHV-1000), and each reported value is an average of five measurements.

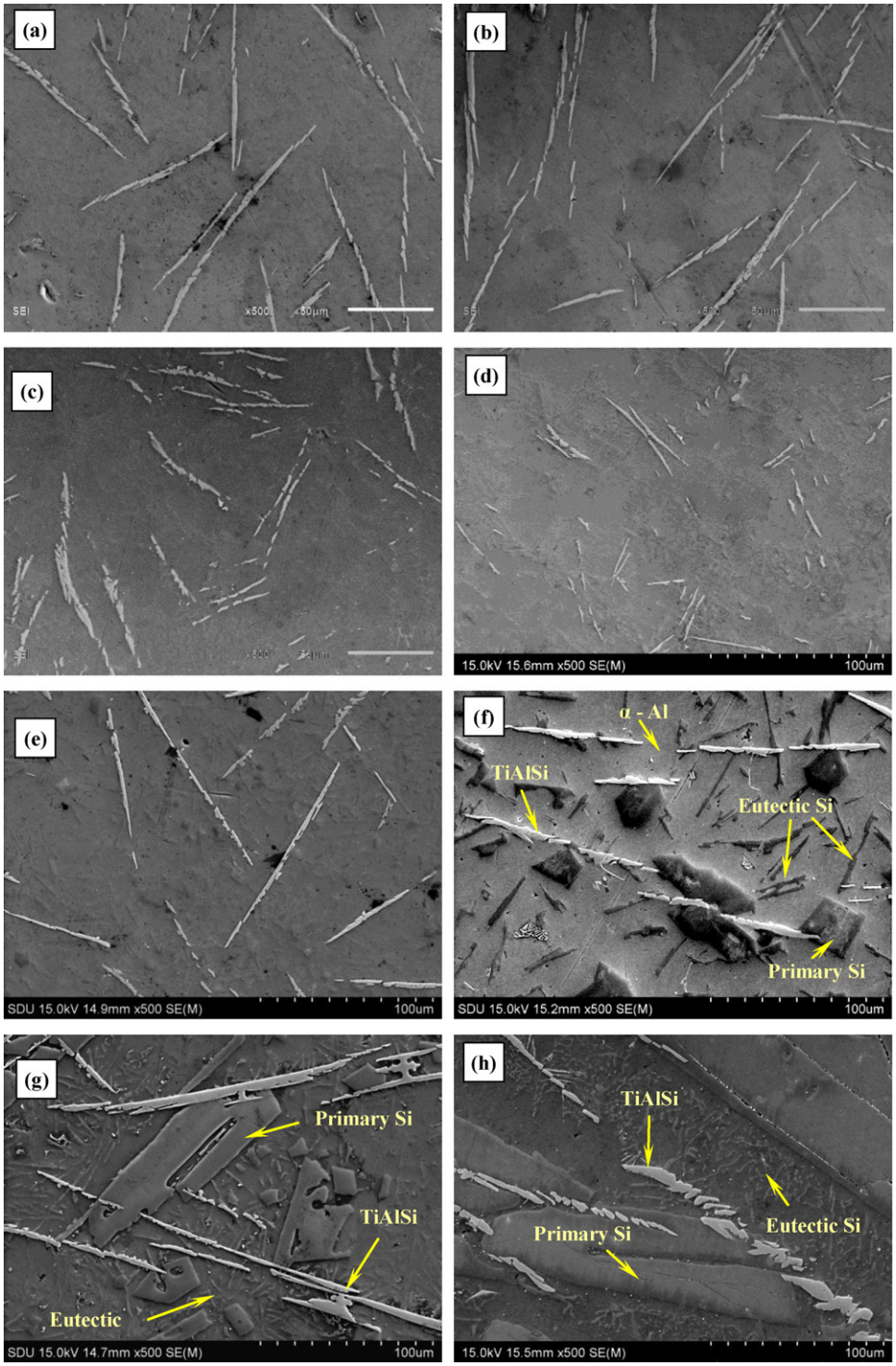

Fig. 2. FESEM microstructures of as-cast Al–Si–2Ti alloys: (a) 3% Si, (b) 6% Si, (c) 10% Si, (d) 12% Si, (e) 14% Si, (f) 18% Si, (g) 30% Si, (h) 60% Si.

Table 1
Chemical compositions and UTS of alloys.

Alloy grades	Elements (wt.%)									UTS (MPa)	δ (%)	$\sigma_{p0.05}$ (MPa)
	Si	Ni	Cu	Fe	Mg	Mn	Zn	Ti	Al			
Group 1	13.0	2.0	3.8	0.5	1.0	0.2	0.1	0.1	Bal.	75.04	4.09	73.98
Group 2	13.0	2.0	3.8	0.5	1.0	0.2	0.1	3.1	Bal.	83.97	4.81	81.48

Each value of UTS, δ and $\sigma_{p0.05}$ is an average of four measurements tested at 350 °C.

Table 2
at.% of Al, Si and Ti in TiAlSi phase.

Alloys	at.%		
	Al	Si	Ti
Al–3Si–2Ti	69.36	6.77	23.87
Al–6Si–2Ti	66.16	10.29	23.55
Al–10Si–2Ti	61.72	14.85	23.43
Al–12Si–2Ti	61.94	15.07	22.99
Al–14Si–2Ti	16.06	53.21	30.73
Al–18Si–2Ti	14.48	54.59	30.93
Al–30Si–2Ti	8.34	60.60	31.06
Al–60Si–2Ti	6.66	61.58	31.76

Each value is an average of five measurements.

3. Results

The microstructures of Al–*x*Si–2Ti alloys are shown in Fig. 2, in which the TiAlSi intermetallics exhibit flake-like. The compositions of TiAlSi in Al–*x*Si–2Ti alloys tested by EDS are shown in Table 2. It is found that the percentage of Si in TiAlSi increases with Si content in the alloys gradually and has a sharp increase at 14% Si. XRD results are shown in Fig. 3, it can be seen that the TiAlSi intermetallics are identified as $Ti(Al_{1-x}Si_x)_3$ in Fig. 3(a)–(d). The $Ti(Al_{1-x}Si_x)_3$ phase maintains the crystal structure of $TiAl_3$. Some Si atoms take the place of Al atoms in $TiAl_3$ lattice structure, leading to alterations of lattice parameters, thus a continuous peak shift was detected. The solubility of Si in $TiAl_3$ is 15.07 at.% in Al–12Si–2Ti alloy shown in Table 2. According to Mondolfo [15], up to 15 at.% Al can be replaced by Si in $TiAl_3$ lattice structure, resulting in various chemical compositions and a range of lattice parameters. Zhu et al. [16] calculated the site preference of Si in $TiAl_3$ using a first principles method and pointed out that the limited solubility of Si in $TiAl_3$ lies between 12.5 at.% and 18.75 at.%. The experimental result in this paper is in agreement with previous results.

The TiAlSi phase transforms to $Ti_7Al_5Si_{12}$ in Al–14Si–2Ti alloy identified in Fig. 3(e). Increasing Si level to 18%, 30% and 60%, the phase still keep as $Ti_7Al_5Si_{12}$. Just as what mentioned above, an increase of Si content in $Ti_7Al_5Si_{12}$ phase as well as the continuous peak shift in the XRD results in Fig. 3(e)–(h) were also detected.

P. Perrot [17] has reported that three possible types of titanium aluminides could be present at the aluminum-rich corner: $Ti(AlSi)_3$, τ_1 and τ_2. $Ti(AlSi)_3$ was written as $Ti(Al_{1-x}Si_x)_3$ in this paper, while τ_1 and τ_2 are commonly written as $Ti_7Al_5Si_{12}$ and $Ti(AlSi)_2$. In this study, we detected the phase evolution from $Ti(Al_{1-x}Si_x)_3$ to $Ti_7Al_5Si_{12}$ at 14 wt.% Si and the increase of Si content in TiAlSi phase with Si level in the alloy, but no $Ti(AlSi)_2$ phase was detected. Since Al and Si can replace each other over a wide range in these phases [17], it results in a large variety of chemical compositions of TiAlSi phases. Thus, the titanium aluminides are generally referred to as TiAlSi intermetallics in many references [9], and that's why the content of Si in $Ti(Al_{1-x}Si_x)_3$ or $Ti_7Al_5Si_{12}$ phase can vary over a wide range in this article.

Titanium aluminides are regarded as relatively hard-phases [18], thus the formation of TiAlSi can lead to the microhardness increase of Al–Si alloy. But the study of microhardness on TiAlSi phase has never been reported so far. In this paper, we tested the microhardness of TiAlSi intermetallics and found its relationship with Si content in Al–*x*Si–2Ti alloys, and the results are shown in Fig. 4. It shows that the increase of Si content in the alloy results in an increase in microhardness values of TiAlSi phase. This is due to the increase of Si content in TiAlSi.

Fig. 5 shows the microstructures of as-cast Al–18Si–2Ti, 4Ti and 5Ti alloys. The TiAlSi phase exhibits flake-like in Fig. 5(a), while exhibits block-like in (c). Besides, we can see that there are almost no primary Si particles in Al–18Si–5Ti alloy. Since the precipitation temperature of TiAlSi intermetallics is higher than that of primary Si [9], TiAlSi phase forms first at the solidification process, thus the

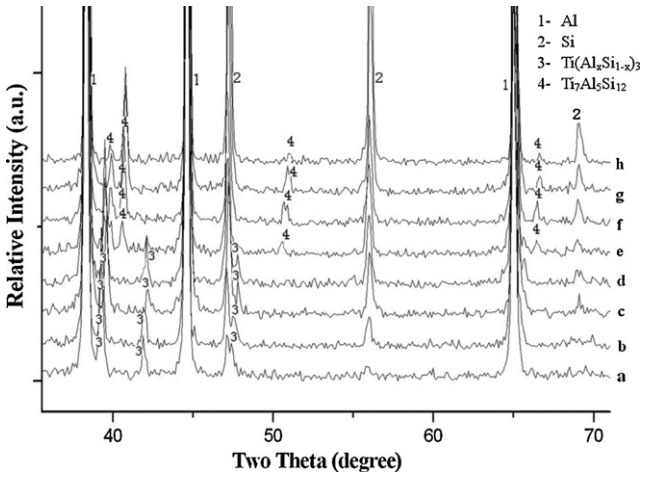

Fig. 3. XRD of as-cast Al–Si–2Ti alloys: (a) 3% Si, (b) 6% Si, (c) 10% Si, (d) 12% Si, (e) 14% Si, (f) 18% Si, (g) 30% Si, (h) 60% Si.

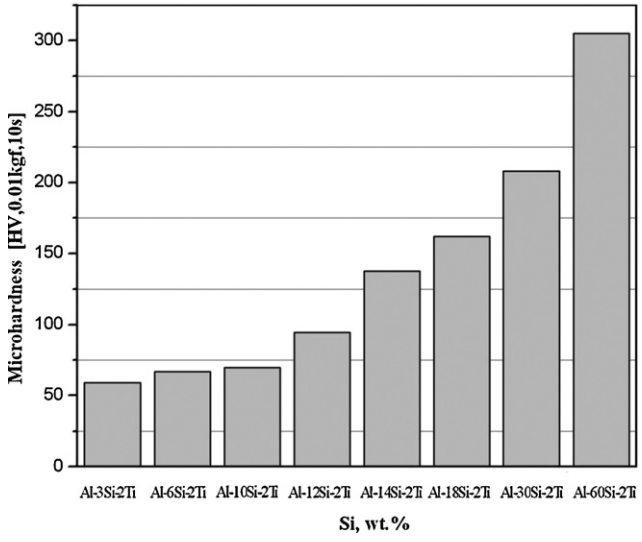

Fig. 4. Graphical representation of the microhardness values of TiAlSi phase in Al–*x*Si–2Ti alloys in the as-cast condition.

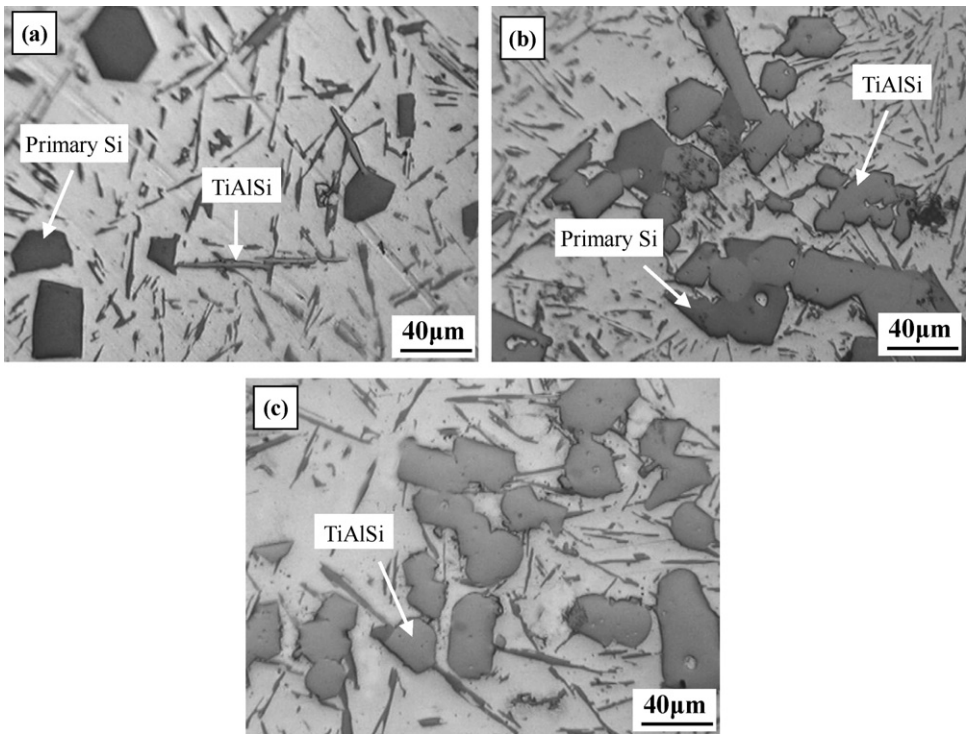

Fig. 5. Microstructures of as-cast Al–18Si–Ti alloys: (a) 2% Ti, (b) 4% Ti, (c) 5% Ti.

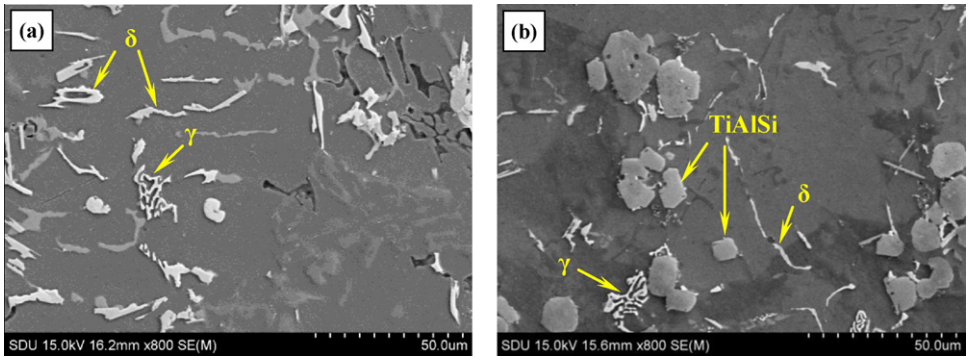

Fig. 6. FESEM micrographs of the piston alloys without and with extra Ti addition after heat-treatment: (a) without extra Ti addition; (b) with extra 3% Ti addition.

increase of Ti content in the alloy will promote the replacement of primary Si by TiAlSi particles. It is known that angular primary Si particles dissever the matrix, leading to a decrease of strength and elongation [19]. Since the blocky TiAlSi particles have no sharp edges, it may lead to improvements of elongation and ductility as well as a decrease of brittleness of the alloy. What's more, the experimental results provide a method to modify primary Si particles in hypereutectic Al–Si alloy by adding Ti.

TiAlSi intermetallics were supposed to have strengthening effect at high-temperature, thus the ultimate tensile strengths (UTS) at 350 °C of a piston alloy containing blocky TiAlSi particles was tested. Respectively, Fig. 6(a) and (b) show heat-treated microstructures of the piston alloy without and with TiAlSi particles. We can see: except for the main heat-resistance phases δ-Al_3CuNi and γ-Al_7Cu_4Ni in Fig. 6(a), blocky TiAlSi particles with the size of 20–30 μm are contained in (b). The alloy composition, UTS, δ and $\sigma_{p0.05}$ are shown in Table 1. It shows that UTS of the piston alloy without TiAlSi particles is 75.04 MPa while is 83.97 MPa after extra 3% Ti addition, thus is increased by 11.9%. The elongation and yield strength shows 17.6% and 10.1% increase respectively after adding extra 3% Ti.

4. Conclusion

Increase of Si level in Al–Si–Ti alloys leads to an increase of Si content in TiAlSi intermetallics. The TiAlSi phase evolves from $Ti(Al_{1-x}Si_x)_3$ to $Ti_7Al_5Si_{12}$ phase at about 14 wt.% Si, while all the TiAlSi intermetallics exhibit flake-like. The limited solubility of Si in $TiAl_3$ is about 15.07 at.%.

By increasing Si content, microhardness of TiAlSi increases synchronously. It is found that increasing Si content from 3% to 60%, microhardness of TiAlSi in Al–*x*Si–2Ti alloys increases from 59.06HV to 305.1HV.

The increase of Ti content in Al–Si–Ti alloys promotes the morphological transformation of TiAlSi from flake-like to block-like and primary Si can be replaced by blocky TiAlSi particles in hypereutectic Al–Si alloy. It can be a new method to modify primary Si particles in hypereutectic Al–Si alloy by adding Ti.

Blocky TiAlSi particles prove to be helpful to enhance the high-temperature strength of an Al–Si piston alloy in this article, which is increased by 11.9%. The elongation and yield strength are increased by 17.6% and 10.1%, respectively.

Acknowledgements

We gratefully acknowledge the support of National Science Fund for Distinguished Young Scholars of China under project 50625101, National Natural Science Foundation of China under project 51071097.

References

[1] L. Lasa, J.M. Rodriguez-Ibabe, J. Mater. Charact. 48 (2002) 371–378.
[2] S. Tomida, K. Nakata, S. Shibata, et al., Surf. Coat. Technol. 169–170 (2003) 468–471.
[3] W. Reif, J. Dutkiewicz, R. Ciach, et al., Mater. Sci. Eng. A 234–236 (1997) 165–168.
[4] G.S. Vinod Kumar, B.S. Murty, M. Chakraborty, J. Alloys Compd. 396 (2005) 143–150.
[5] K.P. Rao, Y.J. Du, Mater. Sci. Eng. A 277 (2000) 46–56.
[6] Ch.H. Liao, Y. Sun, G.X. Sun, J. Mater. Sci. 37 (2002) 3489–3495.
[7] L.N. Yu, X.F. Liu, Zh.Q. Wang, et al., J. Mater. Sci. 40 (2005) 3865–3867.
[8] D. Qiu, J.A. Taylor, M.-X. Zhang, et al., Acta Mater. 55 (2007) 1447–1456.
[9] X.G. Chen, M. Fortier, J. Mater. Process. Technol. 210 (2010) 1780–1786.
[10] M. Zeren, E. Karakulak, Mater. Sci. Technol. 25 (2009) 1211–1214.
[11] N. Saheb, T. Laoui, A.R. Daud, et al., Wear 249 (2001) 656–662.
[12] J. Gröbner, D. Mirković, R. Schmid-Fetzer, Mater. Sci. Eng. A 395 (2005) 10–21.
[13] S. Liu, F. Weitzer, J.C. Schuster, et al., Int. J. Mater. Res. 99 (2008) 705–711.
[14] M. Zeren, E. Karakulak, J. Alloys Compd. 450 (2008) 255–259.
[15] L.F. Mondolfo, Aluminium Alloys: Structure and Properties, Butterworths, London, 1976, pp. 385–387.
[16] G.L. Zhu, D. Shu, Y.B. Dai, et al., Acta Phys. Sin. 58 (2009) S210–S215 (in Chinese).
[17] P. Perrot, in: G. Petzow, G. Effenberg (Eds.), Ternary Alloys – A Comprehensive Compendium of Evaluated Constitutional Data and Phase Diagrams, vol. 8, VCH Publishers, New York, 1990, pp. 283–290.
[18] M.Y. Nazmy, in: N.S. Stoloff, V.K. Sikka (Eds.), Physical Metallurgy and Processing of Intermetallic Compounds, Chapman & Hall, New York, 1996, p. p120.
[19] Y.P. Wu, Sh.J. Wang, H. Li, et al., J. Alloys Compd. 477 (2009) 139–144.